

Received June 27, 2020, accepted July 13, 2020, date of publication July 16, 2020, date of current version July 28, 2020.

Digital Object Identifier 10.1109/ACCESS.2020.3009851

An Adaptive Terrain-Dependent Method for SRTM DEM Correction Over Mountainous Areas

CUI ZHOU¹, GUI ZHANG¹, ZEFA YANG², (Member, IEEE),
MINSI AO³, ZHIWEI LIU², AND JIANJUN ZHU²

¹Key Laboratory for Digital Dongting Lake Basin of Hunan Province, College of Science, Central South University of Forestry and Technology, Changsha 410001, China

²School of Geosciences and Info-Physics, Central South University, Changsha 410083, China

³Hunan Engineering and Research Center of Natural Resource Investigation and Monitoring, Changsha 410007, China

Corresponding authors: Cui Zhou (cuizhou@163.com), Gui Zhang (csfu3s@163.com), and Zefa Yang (yangzf@csu.edu.cn)

This work was supported in part by the Young Elite Scientists Sponsorship Program by Hunan province of China under Grant 2018RS3093, in part by the National Natural Science Foundation of China under Grant 41604012, in part by the China Postdoctoral Science Foundation under Grant 2017M612604, in part by the Hunan Science and Technology Innovation Platform and Talent Plan Project under Grant 2017TP1022, and in part by the Opening Foundation of Hunan Engineering and Research Center of Natural Resource Investigation and Monitoring under Grant 2020-13.

ABSTRACT This paper presents a terrain-related method to simultaneously correct the global error trends and local linear/nonlinear terrain-related errors of the Shuttle Radar Topography Mission (SRTM) digital elevation model (DEM), which have not been focused in most of the previous methods. To meet this goal, an adaptive strategy for modelling the SRTM DEM errors is first proposed, especially over mountainous areas, based on the Bayesian information criterion. Then, the M-estimator, instead of the ordinary least squares solver, is utilized to estimate the model parameters of the constructed model to improve the estimation robustness. The proposed method was tested over the Zhangjiajie areas of China, where the ground surface terrain varies from plains to steep mountains. The results show that the errors of the SRTM DEM over the region of interest decrease from 10.1 m to approximately 8.1 m after correction with the proposed method, indicating an improvement of approximately 20%. In addition, compared with two existing and common methods that can respectively correct the global error trends and local linear terrain-related errors of the SRTM DEM, the accuracy of the corrected SRTM DEM improves by approximately 29% and 27.9% over mountainous areas with slopes larger than 20° when the proposed method is used. Moreover, the proposed method will be beneficial to the correction of other airborne or spaceborne DEM products, especially over mountainous areas.

INDEX TERMS SRTM DEM, global error trends, local nonlinear terrain-related errors, adaptive model, robust estimation.

I. INTRODUCTION

Digital elevation model (DEM) products play an essential role in many studies and practical applications, such as in geophysics, geology, hydrology, geodesy, and urban engineering. Traditionally, DEM products are usually generated by point-based geodetic surveys (e.g., GPS and precise leveling) that are characterized by small working areas, coarse spatial resolution, and large time consumption. In recent decades, advances in remote sensing have dramatically promoted the progress of DEM generation such as using airborne light detection and ranging (LiDAR), spaceborne optical photogrammetry [1], [2] and airborne/spaceborne interferometric synthetic aperture radar (InSAR) [3], [4].

The associate editor coordinating the review of this manuscript and approving it for publication was Jenny Mahoney.

Among these methods, InSAR can generate DEMs with some advantages, such as all-day, all-weather, and high spatial resolution observations. Notably, the Shuttle Radar Topography Mission (SRTM) generated a near-global DEM (80% of the Earth's land area between 56°S and 60°N) with a spatial resolution of approximately 30 m from 11 to 22 February 2000 using airborne C- and X-band SAR sensors [3]. The SRTM DEM is the first near-global homogeneous, high spatial resolution DEM product. Owing to this advantage, the SRTM DEM product has been widely applied in numerous fields until now, such as geology, geomorphology, glaciology, natural hazard evaluation, and vegetation survey studies (e.g., [5]–[11]), although the product was generated 20 years ago.

To guide the applications of this type of product, the accuracy of the SRTM DEM has been extensively assessed using

elevation measurements acquired by global position system (GPS) receivers, corner reflector arrays, ocean data, and other DEM products such as optical-based DEMs and airborne DEMs [12]–[14]. The results suggest that the absolute vertical error is generally smaller than 16 m, and the absolute error of circular geolocation is less than 20 m [3]. It is noted, however, that such an accuracy performance usually occurs in plain and low vegetated areas. In regard to mountainous areas and/or densely vegetated areas, the accuracy of the SRTM DEM is significantly degraded (e.g., dozens of or even hundreds of metres in elevation) [15], [16]. Previous studies have suggested that there are three main components of SRTM DEM errors over mountainous areas, in addition to random errors (can be reduced by filtering): i) vegetation biases due to the weak penetration of the X- or C-band microwave sensors into forests [17], ii) global (or long-wavelength) error trends [18], and iii) terrain-related (e.g., height, slope and aspect) errors [12], [14], [19].

In recent decades, great efforts have been made to improve the accuracy of the SRTM DEM (hereafter referred to as SRTM DEM correction) over vegetation areas by mitigating vegetation biases using multi-source raster/surface data (e.g., spaceborne and/or airborne LiDAR and remote sensing images) (e.g., [17], [20], [21]). Generally, the vegetation biases and the remaining two error sources of the SRTM DEM can be effectively mitigated (e.g., on the order of a few metres) if dense elevation measurements of the “bare” ground surface are available (e.g., obtained by LiDAR). Therefore, the removal of the vegetation biases would not be discussed in this paper. As for the two remaining main error sources, a widely-used strategy for reducing them is fusing point-wise height observations with higher accuracy (e.g., obtained by GPS and/or ICESat) than the SRTM DEM [14], [22].

The core idea behind the widely-used strategy is that firstly generating the differences between the point-wise height observations and the corresponding SRTM DEM. Artificial intelligence techniques (e.g., artificial neural network) [23], [24] or mathematical models [14], [22] are then used to forward correct the errors of the SRTM DEM. In which, the mathematical model-based correction is common to use in practice, owing to the explicit relationship between the SRTM DEM errors and the affected factors. There are two common mathematical models used for SRTM DEM correction: i) a spherical harmonics model (SHM) for correcting global error trends and ii) multiple linear regression (MLR) models that relate the local terrain-dependent errors to surface terrain factors (e.g., heights, slopes and aspects). However, these two models have some disadvantages. For instance, the SHM cannot consider the local terrain-dependent errors; thus, it is usually used over relatively flat areas. The MLR model considers the linearly local terrain-dependent errors but does not consider the global error trends, degrading the accuracy of the corrected SRTM DEM. Moreover, the non-linear components of the local terrain-dependent errors do not be taken into account in

the MLR method. These two limitations would degrade the performance of the MLR method, especially over mountainous areas where nonlinear terrain-dependent errors exist in the SRTM DEM. To the best of our knowledge, models that simultaneously consider global trends and local terrain-dependent linear/nonlinear errors of SRTM DEMs are currently lacking.

In this paper, we proposed an adaptive method for SRTM DEM correction over mountainous areas by simultaneously considering the global error trends and local terrain-dependent errors. This method can adaptively model the linear/nonlinear terrain-related errors of the SRTM DEM over mountainous areas based on the Bayesian information criterion (BIC). In doing so, the MLR model is taken as a specific case of the proposed model. In addition, the proposed method estimates the model parameters using a robust estimation solver (i.e., M-estimator) instead of the ordinary least squares (LS) solver used in the SHM and MLR methods to improve the estimation robustness. Finally, the proposed method was tested over the Zhangjiajie area of China.

II. METHODOLOGY

A. OVERVIEW OF THE SHM AND MLR MODEL

1) OVERVIEW OF THE SHM

According to Wendleder *et al.* [18], the global error trends are dependent on the geological longitudes (namely E) and latitudes (namely N) of the SRTM DEM; thus, a spherical harmonics model (SHM) is selected to model the error trend f_{trend} , i.e.,

$$f_{trend}(E, N) = \sum_{n=0}^{\infty} \sum_{m=0}^n A_{nm} R_{nm}(E, N) + B_{nm} S_{nm}(E, N) \quad (1)$$

where A_{nm} and B_{nm} are the dimensionless weighting coefficients; R_{nm} and S_{nm} are the surface spherical harmonics; and m and n are the degree and order of the SHM.

2) OVERVIEW OF THE MLR MODEL

The MLR method corrects the local terrain-related errors of the SRTM DEM by constructing a multiple linear regression analysis as

$$\Delta H = a_0 + a_1 S + a_2 A + a_3 H \quad (2)$$

where ΔH is the elevation differences between the SRTM DEM elevations and the in situ measurements obtained by levelling, GPS, or even ICESat measurements at the field points; S , A and H are the corresponding slopes, aspects, and SRTM DEM elevations of the in situ locations; and $\mathbf{P} = [a_0, a_1, \dots, a_3]^T$ represents the model parameters for the MLR model. Then, the unknown \mathbf{P} values are determined with effective in situ elevation measurements using a LS solver. Finally, the SRTM DEM elevation can be corrected pixel-by-pixel based on Equation (2). The global trend errors and high-order terrain-related errors cannot be taken into account by the MLR model. As a consequence, the accuracy

of the corrected SRTM DEM would be degraded, especially over mountainous areas where nonlinear terrain-related errors exist.

B. DEVELOPMENT OF THE ADAPTIVE TERRAIN-DEPENDENT METHOD

As stated previously, the SRTM DEM contains three major error sources (i.e., vegetation biases, global trend errors, and local terrain-related errors). Hence, the difference vector between the SRTM DEM elevation and in situ elevation measurements, namely, ΔH , can be expressed as

$$\Delta H = f_{trend}(E, N) + f_{terrain}(S, A, H) + \Delta h + \delta \quad (3)$$

where E, N, H, S , and A are the vectors of the longitudes, latitudes, elevations, slopes, and aspects of the SRTM DEM at the collected field points; Δh denotes the corresponding vegetation biases, and δ is the residual error term. f_{trend} and $f_{terrain}$ denote the mapping functions of geolocation-related (or global trend) errors and terrain-dependent errors. As previously stated, the correction of vegetation biases of the SRTM DEM generally requires in situ “bare” Earth measurements that are usually unavailable in most cases. Consequently, we allow the error component of vegetation biases alone and only correct the first two error components in this study. At this stage, the key of the proposed method is to construct explicit models of the mapping functions of f_{trend} and $f_{terrain}$.

1) MODEL CONSTRUCTION FOR GLOBAL TREND ERROR CORRECTION

A geolocation-related linear model was constructed to model the global trend errors in this study according to [15], i.e.,

$$f_{trend}(E, N) = a_0 + a_1 \sin E + a_2 \cos(90^\circ - N) \quad (4)$$

with a_0, a_1, a_2 being the model parameters. Unlike the SHM presented by Wendleder *et al.* [18] (see Equation (1)), the presented new model (i.e., Equation (4)) is consists of two parts, i.e., a constant term (i.e., a_0) and a special harmonics model term with the maximum degree of one (i.e., $a_1 \sin E + a_2 \cos(90^\circ - N)$). In doing so, global trend errors in SRTM DEM over a small area (extremely trended to a constant) can be modelled. However, it should be pointed out that, as suggested by Wendleder *et al.*, a SHM with high degrees (i.e., Equation (1)), rather than Equation (4), is preferred to be used to correct the global trend errors in SRTM DEM over a large area (regional or continental scale).

2) BIC-BASED MODEL CONSTRUCTION FOR LOCAL TERRAIN-RELATED ERROR CORRECTION

Previous studies have suggested that the terrain-dependent errors of the SRTM DEM products are mainly dependent on the heights, slopes, and aspects of surface terrain [12], [14], [19]. A linear relationship between the errors with respect to the heights was revealed. Consequently, to better correct the terrain-dependent errors, the new terrain-related

errors in Equation (3), namely, $f_{terrain}$, are constructed as

$$f_{terrain}(S, A, Z) = a_3 H + f_{TF}(S, A) \quad (5)$$

where a_3 is the coefficient of height-related errors of the SRTM DEM, and $f_{TF}(S, A)$ represents the slope- and aspect-related errors. The correction function of $f_{TF}(S, A)$ was designated by a linear model with respect to the slopes and aspects in the MLR method. However, a linear (one-order) model is unsuitable for mountainous areas where a high-order (nonlinear) model can only describe the terrain-related errors of the SRTM DEM.

To circumvent this shortcoming, an adaptive strategy is proposed to determine the order of $f_{TF}(S, A)$ in this study. More specifically, we first generate a finite set of polynomials with varying orders (usually one to five) with respect to slopes and aspects. Note that it is possible to increase the likelihood of improving data fitting by adding parameters when fitting the models, but doing so may result in overfitting. The BIC resolves this problem by introducing a penalty term for the number of parameters in the model. The BIC is mathematically defined as

$$BIC = \ln(n)k - 2L \quad (6)$$

where n denotes the observation sample size, k is the number of independent parameters, and L is the log-likelihood of the model. Then, the model achieving the lowest BIC value is chosen as the best model for describing the slope- and aspect-related errors of the SRTM DEM. Due to the use of BIC, the proposed method can construct an adaptive model for SRTM DEM error correction. We take the polynomial involving two-order slope and four-order aspect as an example. The complete terrain-dependent model constructed by the proposed method can be expressed as

$$\Delta H = \begin{bmatrix} 1 & \sin E & \cos(90^\circ - N) & H & S & A & S^2 & SA \end{bmatrix} \begin{bmatrix} a_0 \\ a_1 \\ \vdots \\ a_{14} \end{bmatrix} \quad (7)$$

To simplify the following statement, we rewrite Equation (7) with a matrix formation as

$$\Delta H = B \cdot X \quad (8)$$

where X denotes the model parameters, and B denotes the model factor vectors. Note that the MLR method (Equation (2)) is a special case of Equation (8) where the remaining parameters are all zeros, except for a_0 and $a_3 \sim a_5$. It should be pointed out that the vegetation biases in SRTM DEM are dependent on the terrain-related errors. Therefore, Equation (8) is likely to correct the hybrid errors in SRTM DEM associated with vegetation and surface terrain, instead of the terrain-related errors only, especially over those mountainous areas covered by vegetation.

C. ROBUST ESTIMATION OF PARAMETERS OF THE TERRAIN-DEPENDENT MODEL

In addition to model errors, the accuracy of the corrected SRTM DEM primarily depends on the uncertainties of the parameter estimates. Differentiating from the previous SHM and MLR methods where the LS solver is used, the proposed method estimates the parameters of the constructed terrain-dependent model using robust estimation due to the following factors. The parameters are estimated using in situ elevation measurements that may contain gross errors (i.e., very large errors), thereby dramatically reducing the accuracy or even causing an incorrect result for the corrected SRTM DEM. Consequently, it is essential to mitigate the influence of gross errors. In addition, when in situ elevation measurements are observed by different techniques, such as GPS, precise levelling, and ICESat, it is crucial to designate suitable weights for in situ elevation measurements to improve the accuracy of the model parameter estimates.

The robust estimation methods are capable of retrieving robust solutions by adaptively designating weights for the observations. Hence, we select the M-estimator [25], [26], a widely used robust estimation method, to estimate the model parameters of the constructed model. The robust solutions of the model parameter vector \hat{X} can be obtained from Equation (8) by iteratively reweighting the following equation:

$$\hat{X}^{k+1} = [B^T P^k B]^{-1} B^T P^k \Delta H \tag{9}$$

until $\|\hat{X}^{k+1} - \hat{X}^k\|$ is smaller than a designated threshold (e.g., 10^{-4}). Let the number of in situ elevation measurements be n . Thus, the weighting matrix $P^k = \text{diag}[P_1^k, P_2^k, \dots, P_n^k]$ in the k th iteration can be determined by [27]

$$P_k^{(i)} = \begin{cases} 1, & |\mu_k^{(i)}| \leq b \\ b / |\mu_k^{(i)}|, & b < |\mu_k^{(i)}| \leq c \\ 0, & |\mu_k^{(i)}| > c \end{cases} \tag{10}$$

where $P_k^{(i)}$ denotes the i main diagonal entry of P^k , $\mu_k^{(i)} = e_k^{(i)} / \delta_k$ is the standardized residual with $e_k^{(i)}$ being the residual of the i th observation equation and δ_k being the standard deviation of the k th iteration, and b and c are constants (usually designated as 1.5 and 2.5, respectively).

Equation (10) indicates that, for an observation with a gross error (i.e., $|\mu_k^{(i)}| > c$), the M-estimator can designate a zero weight to remove its contribution to the model parameter estimation, avoiding the influence of gross errors on the model parameter estimates. In addition, the M-estimator can adaptively designate weights to other observations without prior weight information that the previous LS solver cannot achieve, thereby improving the accuracy of the model parameter estimates. It should be pointed out that the independent variables in Equation (8) (i.e., B) have different units,

such as degrees for longitude and latitude and metres for height. Therefore, prior to model estimation, the normalization of these independent variables must be conducted.

$$B' = 2 * \frac{B - \min(B)}{\max(B) - \min(B)} - 1 \tag{11}$$

where B' is the normalized value of the variable B .

D. SRTM DEM CORRECTION WITH THE TERRAIN-DEPENDENT MODEL

With the robust estimates of the model parameters \hat{X} , the pixelwise correction of the SRTM DEM \hat{H} can be achieved by

$$\hat{H} = H_1 + B_1 \cdot \hat{X} \tag{12}$$

where H_1 is the elevation vector of the SRTM DEM at each pixel and B_1 is the coefficient matrix involving the new independent variables (e.g., longitudes, latitudes, elevation slopes, and aspects) of the SRTM DEM at each pixel. The flowchart of the proposed method is shown in Figure 1.

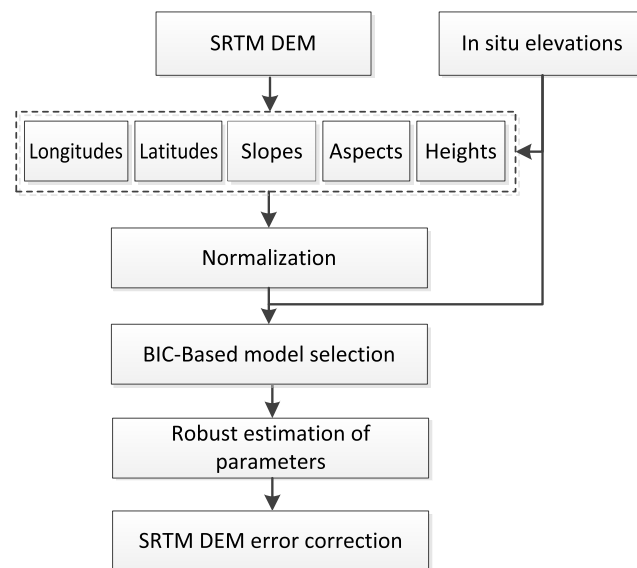


FIGURE 1. Flowchart of the proposed method for SRTM DEM correction.

III. EXPERIMENTS AND RESULTS

A. STUDY AREA AND DATA PROCESSING

The Zhangjiajie area in Hunan Province of China was selected to test the proposed method. Figure 2 shows the SRTM DEM over the selected region of interest (ROI). The terrain in the northern part of the ROI is relatively flat, with elevations varying from approximately 118 to 630 m and slopes ranging from 0° to 13°. The terrain in the southern part is mountainous with elevations ranging from approximately 130 to 1452 m and slopes varying from 0° to 72°. The land cover of the ROI dominates by forestry (about 80%), in addition to residential and agricultural areas. The various types of ground surface terrain in the ROI provide a comprehensive performance evaluation of the proposed method. In addition,

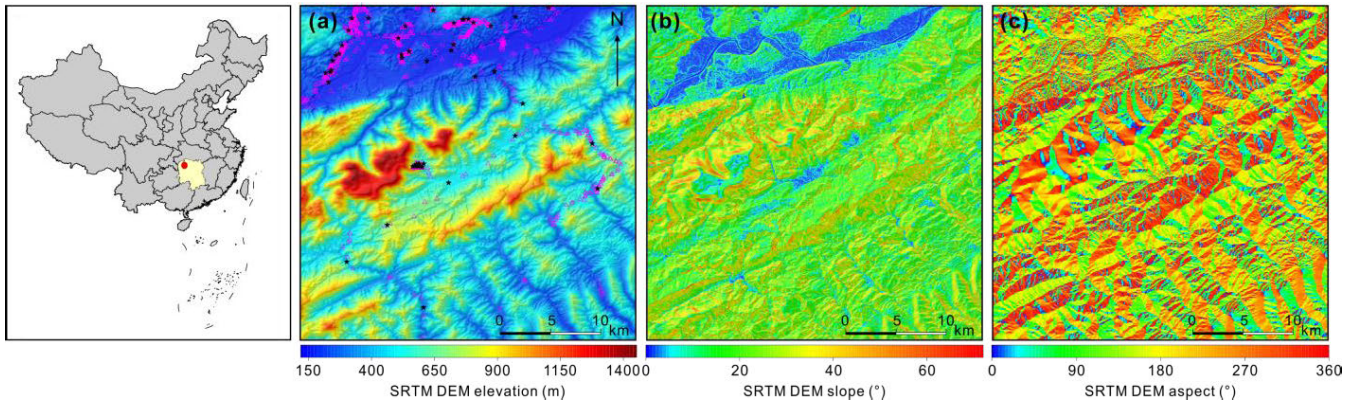


FIGURE 2. Elevations (a), slopes (b), and aspects (c) of the SRTM DEM over the Zhangjiajie area, Hunan Province, China. The magenta triangles and black stars in (a) denote the locations of in situ GPS elevation measurements used for parameter estimation and accuracy validation.

1051 in situ elevation measurements (see the black asterisks and magenta triangles) were collected using either the Continuously Operating Reference Stations of Hunan Province or other GPS surveys. The locations of the 1051 GPS points are marked by black asterisks and magenta triangles in Figure 2. The in situ elevations at these points range from 139 to 939 m. These in situ measurements can provide estimates of model parameters and can be used to evaluate the accuracy of the corrected SRTM DEM.

The GPS elevation measurements refer to the World Geodetic System 84 (WGS 84) geoid (i.e., ellipsoidal height), whereas the SRTM DEM elevations refer to the Earth Gravitational Model 96 (EGM 96) geoid (i.e., orthometric height). Hence, prior to correcting the SRTM DEM, all GPS height measurements in the WGS 84 geoid, namely, H_{WGS84} , were transferred to the EGM 96 geoid (namely, H_{EGM96}) with

$$H_{EGM96} = H_{WGS84} - N \tag{13}$$

where N is the geoid undulation.

B. MODEL CONSTRUCTION OF SRTM DEM ERROR CORRECTION

Figures 3(a) and 3(b) show the errors of the SRTM DEM elevations at the 1051 in situ GPS observation points with respect to the corresponding aspects and slopes. As seen, there are no obvious linear relationships between the SRTM DEM errors and slopes and aspects. The results show that the SRTM DEM errors exhibit a nonlinear relationship with respect to the slopes and aspects. To model the SRTM DEM errors as accurately as possible, Equation (4) is first utilized to model and further remove the global error trends from the SRTM DEM. Then, the BIC-based adaptive strategy described in section II.A is used to model the local terrain-related errors of the SRTM DEM with respect to the heights, slopes and aspects from the residual errors after global error trend removal. The results show that a polynomial with one-order height, two-order slopes, and four-order aspects is the optimized model among all other polynomials. Finally, the BIC-based adaptive model was integrated with

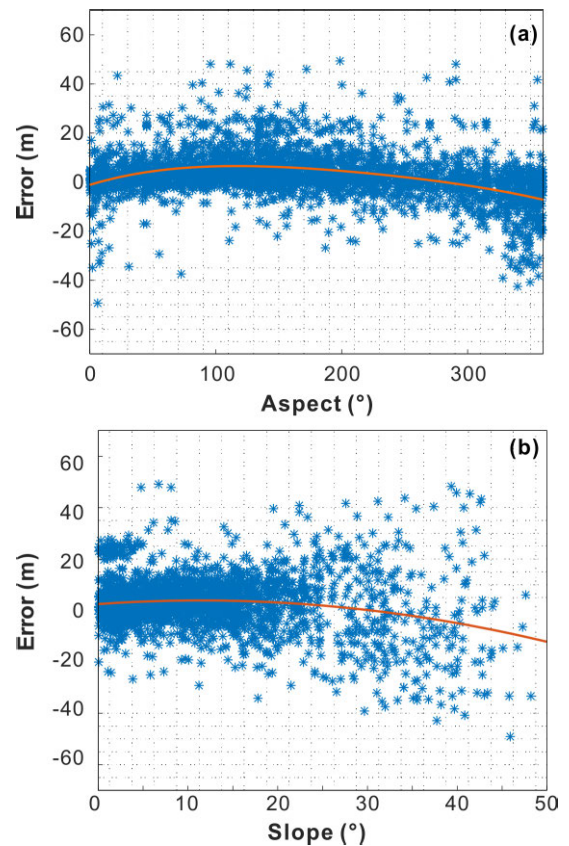


FIGURE 3. The absolute error of the SRTM DEM at the 1001 in situ GPS measurements with respect to aspect (a) and slope (b).

the model for global trend error correction to build the final model (see Equation (7)).

C. PARAMETER ESTIMATION AND ERROR CORRECTION OF SRTM DEM

Prior to SRTM DEM correction, the parameters of the constructed model (i.e., Equation (7)) should be determined. Equation (7) involves 15 model parameters (a_0 to a_{14}); thus, at least 15 effective observations are theoretically required

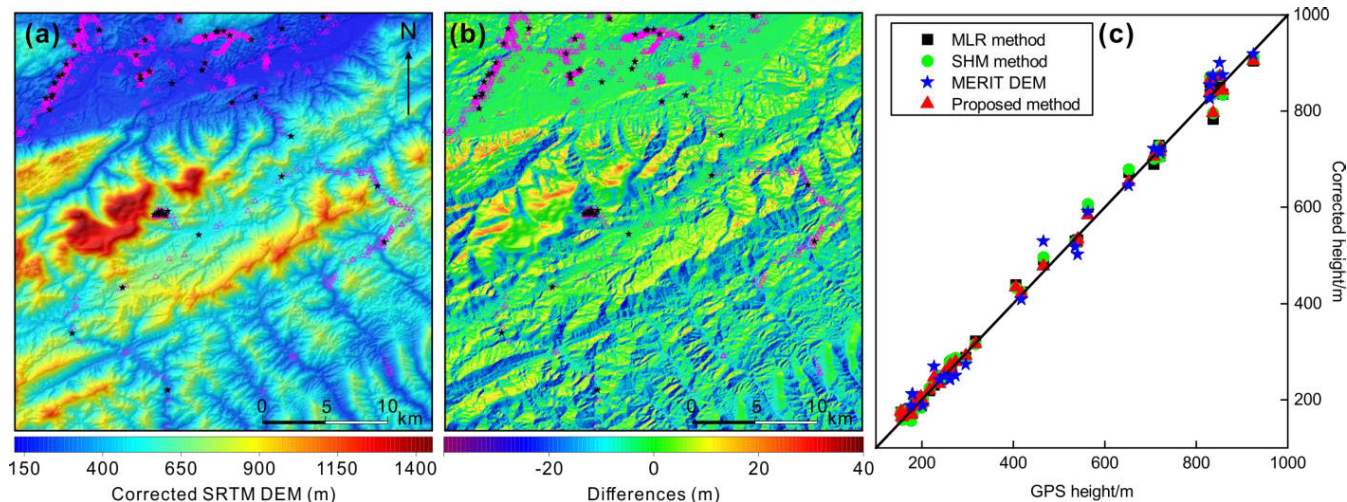


FIGURE 4. (a): Corrected SRTM DEM over the ROI using the proposed method; (b): difference between the corrected and the original SRTM DEM; (c) cross validation between the corrected SRTM DEM and in situ elevations at the 50 GPS heights (their locations are marked by black stars in (a)).

to estimate all of the unknown parameters. In this study, 1051 GPS-measured observations were collected over the ROI, and all of the observations can be theoretically used to model the parameter estimations. However, for the sake of accuracy validation, 50 in situ points (their geolocations are shown by the black stars in Figure 2) with nearly uniform distributions of slopes and aspects were selected. Then, the remaining 1001 in situ measurements were utilized to model the parameter estimations of the constructed model using the M-estimator. Finally, the SRTM DEM correction was conducted pixel-by-pixel based on the constructed model and its parameter estimates.

Figure 4(a) shows the SRTM DEM after correction, and Figure 4(b) shows the difference between the original (see Figure 3(a)) and the corrected SRTM DEM over the ROI. The results show that the maximum difference is approximately -50 m, and the differences are mainly attributed to the local terrain-related errors and global trend errors [28], [29]. To quantitatively evaluate the accuracy of the SRTM DEM error correction, we compared the corrected SRTM DEM elevations with those of the 50 selected in situ points (see red triangles in Figure 4(c)). The result shows a good agreement between both, with an RMSE of approximately 8.1 m, indicating an accuracy improvement of approximately 20% with respect to the RMSE of the SRTM DEM without error correction (i.e., 10.1 m). The results suggest that the proposed method can effectively improve the elevation accuracy of the SRTM DEM.

IV. DISCUSSIONS

A. COMPARISON WITH THE PREVIOUS SHM AND MLR METHODS

We compared the proposed method with the two common mathematical model-based methods, namely, the SHM and MLR methods, in this section. The SRTM DEM was corrected using both the SHM and MLR model based on the

same 1001 in situ GPS measurements. The cross validation of the corrected results with 50 in situ GPS measurements is shown in Figure 4(c) (marked by black rectangles and green circles). In addition, the RMSEs of the SHM- and MLR-corrected SRTM DEM are listed in Table 1. For the sake of comparison, the RMSE of the proposed method is added to this table.

As shown in Table 1, the SHM and MLR methods improved the accuracy of the SRTM DEM with average accuracy improvements of approximately 2% and 4%, respectively. However, the RMSEs of the SHM- and MLR-corrected results were 9.9 and 9.7 m, respectively, greater than that of the SRTM DEM corrected by the proposed method (i.e., 8.1 m). In other words, the accuracy of the method proposed in this study is improved by approximately 18.2% and 16.5% with respect to the accuracies of the SHM and MLR methods.

TABLE 1. Accuracy comparison of the corrected SRTM DEM using the SHM, MLR, and proposed methods.

Items	RMSE (m)				
	Original	SHM	MLR	Proposed	
Averaged	10.1	9.9	9.7	8.1	
Slope intervals	$0 < \text{Slope} \leq 10$	7.8	7.2	7.2	7.1
	$10 < \text{Slope} \leq 20$	8.6	8.2	7.5	6.5
	$20 < \text{Slope}$	17.8	18.6	18.3	13.2

To further analyse the results, we calculated the RMSEs of the corrected SRTM DEM with these three methods at slope intervals of $0^\circ \sim 10^\circ$, $10^\circ \sim 20^\circ$, and $>20^\circ$, and the results are also provided in Table 1. For the slope range of $0^\circ \sim 10^\circ$, the accuracies of the corrected SRTM DEM using the SHM, MLR and the proposed methods are close (i.e., 7.2, 7.2 and 7.1 m, respectively). In regard to the slope range from 10° to 20° , the RMSEs of the SRTM DEM corrected by the SHM and MLR method are 8.2 and 7.5 m, respectively,

while that of the proposed method is approximately 6.5 m, indicating accuracy improvements of approximately 20.7% and 13.3%, respectively. This result is expected because the SHM method does not take terrain-related errors into account. When the slopes of the SRTM DEM are larger than 20° , the RMSEs of the SHM- and MLR-corrected SRTM DEM rapidly increase to 18.6 and 18.3 m, respectively, whereas that of the proposed method slowly increases to 13.2 m, indicating accuracy improvements of approximately 29% and 27.8%, respectively, with respect to the SHM and MLR methods in this study. This result suggests that the proposed method has a better accuracy performance on SRTM DEM correction over mountainous areas (especially for slopes $>20^\circ$).

B. COMPARISON WITH THE MERIT DEM

To further show the advantage of the proposed method, we compared the corrected SRTM DEM using the proposed method with the Multi-Error Removed Improved-Terrain DEM (MERIT DEM) achieved by Yamazaki *et al.* [28]. The comparison with the GPS heights at the selected 50 points shows a RMSE of the MERIT DEM of about 18.3 m, which is higher than the RMSE of 8.1 m obtained in this paper. In addition, the RMSEs of the MERIT DEM for the areas with slope $\leq 10^\circ$, $10^\circ < \text{slope} \leq 20^\circ$, and slope $>20^\circ$ are 6.7, 15.9, and 26.4 m, respectively. The results suggest that the accuracy of the MERIT DEM is slightly higher than the corrected one in this paper (i.e., 7.1 m) in the case of slope $\leq 10^\circ$. However, for those areas with slopes larger than 10° , the accuracy of the MERIT DEM is lower than the corrected ones (i.e., 6.5 m for $10^\circ < \text{slope} \leq 20^\circ$ and 13.2 m for slope $>20^\circ$). This fact, in turn, shows the advantage of the proposed method; that is, it could effectively improve the accuracy of SRTM DEM products, especially over mountainous areas.

The possible reasons for the lower accuracy of the MERIT DEM with slope $>10^\circ$ are analyzed below. Firstly, the MERIT DEM has a spatial $3''$ resolution (about 90 m), which is lower than 30 m SRTM DEM used in this paper. For mountainous areas (e.g., slope $>10^\circ$), spatially averaging 30 m SRTM DEM (the common method for generating 90 m SRTM DEM) to 90 m MERIT DEM would cause errors, even though error correction has been made by Yamazaki *et al.* [28]. Secondly, the lower accuracy may be caused by the extra errors in the data (i.e., tree height bias) used to MERIT DEM correction.

C. INFLUENCE OF TERRAIN-RELATED MODELS ON SRTM DEM CORRECTION

The proposed method develops a BIC-based strategy to adaptively determine the optimized polynomial among a set of polynomials with different orders of slopes and aspects to describe the terrain-related errors of the SRTM DEM. To intuitively show the influence of terrain-related errors on the accuracy of the SRTM DEM correction, we compared the RMSEs of the corrected SRTM DEM by varying only the orders of slopes and aspects in Equation (8), and the results are plotted in Figure 5. The model parameters were determined using the M-estimator based on the 1001 selected in

situ GPS measurements described in Section III.C. As shown in Figure 5, terrain models have a great impact on the accuracy of the SRTM DEM correction. For example, the RMSE is approximately 9.8 m when the linear polynomial with respect to aspect and slope (i.e., the order combination of (1, 1)) was selected. However, the RMSEs gradually decreased when high-order aspects were considered (e.g., 8.2 m for the combination of (1, 5)). When the polynomial with a second-order slope and a fourth-order aspect was selected, the accuracy of the corrected SRTM DEM reached the highest (i.e., approximately 8.1 m) among all other defined order combinations in Figure 5. This result suggests that the developed BIC-based strategy for adaptive model selection is feasible and reliable.

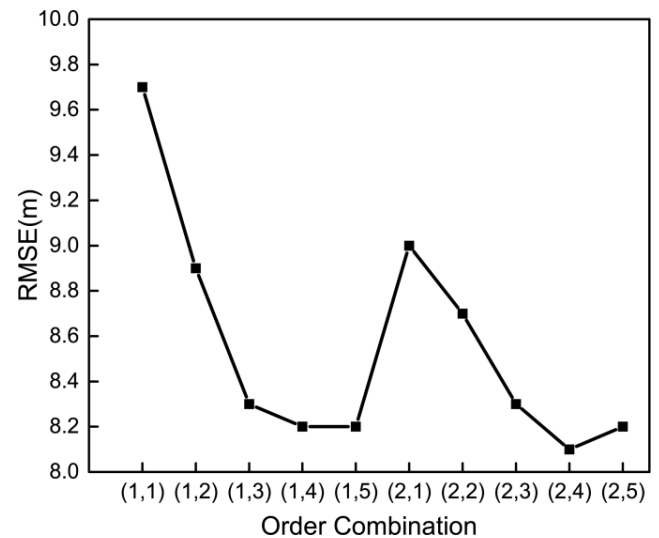


FIGURE 5. Accuracy comparison between the used terrain models that combine different orders of slopes (1 or 2) and aspects (1 to 5).

D. INFLUENCE OF IN SITU MEASUREMENTS ON SRTM DEM CORRECTION

1) INFLUENCE OF GROSS ERRORS OF IN SITU MEASUREMENTS

As stated previously, in situ elevation measurements inevitably contain errors or even possibly gross errors. To mitigate the influence of gross errors, a robust estimator named the M-estimator, instead of the LS solver used in the SHM and MLR methods, is utilized to estimate the model parameters. To intuitively present the influence of gross errors on the SRTM DEM correction using the M-estimator and the LS method, we first randomly selected 1% to 10% (referred to as the percent ratio of gross errors) of the in situ GPS elevations and then randomly added gross errors ranging from 30 to 50 m to the selected GPS points. Then, the M-estimator and LS methods were used to estimate the model parameters for Equation (7). Finally, the SRTM DEM was corrected based on the parameter estimates using the M-estimator and LS solvers. The RMSEs of the corrected SRTM DEM with different percent ratios of gross errors (i.e., from 1% to 10%) using different estimators are plotted in Figure 6.

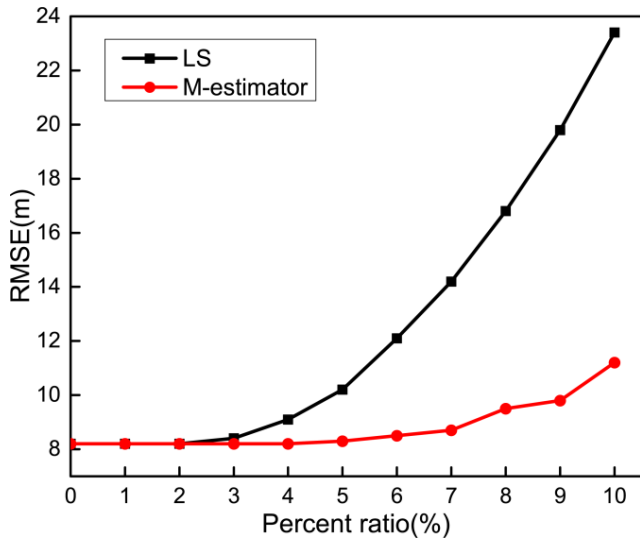


FIGURE 6. Influence of in situ measurements with different errors on SRTM DEM correction.

Figure 6 shows that the RMSEs of the corrected SRTM DEM increase exponentially from approximately 8.1 to 23.4 m as the percent ratios of gross errors increase from 0% (no or a few gross errors) to 10% when the LS method is used. In contrast, the RMSEs gradually increase from 8.1 to 11.2 m when the M-estimator is utilized, indicating an accuracy improvement from 0% to 52.1%. In addition, the RMSEs of the SRTM DEM corrected using the M-estimator remain nearly constant when the percent ratios of gross errors increase from 0% to 6%. This result suggests that the M-estimator can effectively reduce the influence of gross errors when the percent ratios are smaller than 6% in this study.

2) INFLUENCE OF THE NUMBER OF IN SITU MEASUREMENTS

As stated above, the parameters of the constructed model can be theoretically estimated, provided that the number of “effective” in situ measurements is equal to the number of model parameters. The term “effective” means that the features of the selected in situ measurements (e.g., number and

spatial distribution) could mathematically constrain the error trends described by the constructed model if the model error is negligible. In this section, we first discuss the influence of the number of selected in situ GPS measurements on the SRTM DEM correction. More specifically, we formed 25 groups of in situ GPS measurements with varied numbers from 30 to 1000 by considering a normal distribution with respect to both the slopes and aspects. Then, we estimated the model parameters based on these 25 groups of in situ measurements using the M-estimator and forward corrected the SRTM DEM. To reduce randomness, the above steps were repeated 100 times, and the averaged RMSEs of the corrected SRTM DEMs with respect to different numbers of in situ GPS measurements are plotted in Figure 7(a).

As shown, the RMSE of the corrected SRTM DEM was 15.8 m when 30 in situ GPS measurements were selected for model parameter estimation. With an increase in the number to approximately 100, the RMSE exponentially decreases to approximately 9.3 m, showing an accuracy improvement of approximately 8%. With the continual increase in the number to 200, the RMSE decreases to approximately 8.8 m but with a much smaller rate of decrease with respect to that when the number increases from 30 to 100. Following that, the RMSE remains stable at approximately 8.1 m, even though the number increases up to 1000. This result suggests that the number of in situ measurements has a great influence on the SRTM DEM correction. Consequently, it is beneficial to select more available in situ measurements to improve the accuracy of the corrected SRTM DEM using the proposed method.

3) INFLUENCE OF THE SPATIAL DISTRIBUTION OF IN SITU MEASUREMENTS

In this section, the influence of the spatial distribution of in situ measurements on SRTM DEM correction is discussed. To this end, we first divided the 1001 in situ measurements into several groups in accordance with the slope (i.e., <math><5^\circ</math>, <math><10^\circ</math>, <math><15^\circ</math>, <math><20^\circ</math>, <math><25^\circ</math>, <math><30^\circ</math>, <math><35^\circ</math>, <math><40^\circ</math>, and <math><45^\circ</math>) and aspect thresholds (i.e., <math><60^\circ</math>, <math><120^\circ</math>, <math><180^\circ</math>, <math><240^\circ</math>, <math><300^\circ</math>, and <math><360^\circ</math>). To reduce the influence of the number of in situ measurements, we chose 200 GPS measurements (if sufficient) from each group using the following criteria.

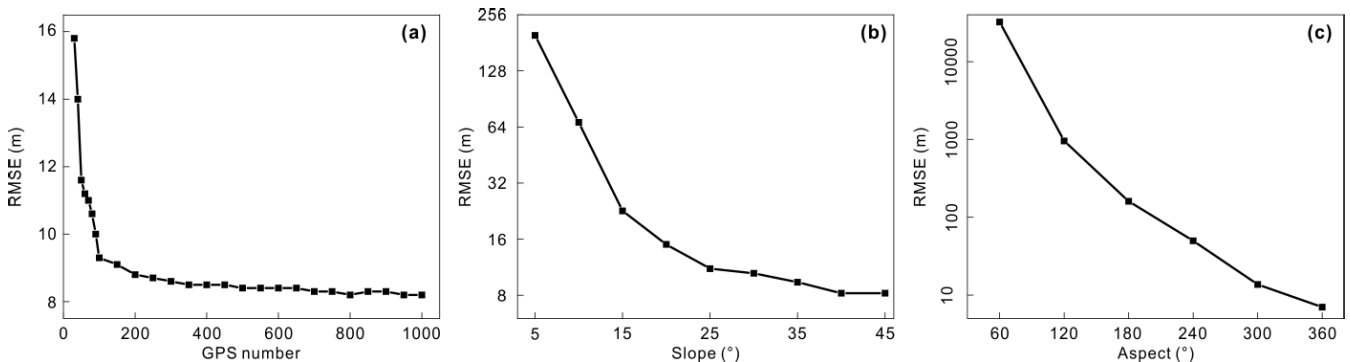


FIGURE 7. Influence of the number (a), slope distribution (b), and aspect distribution (c) of in situ elevation measurements on the accuracy of SRTM DEM correction. Note that a logarithmic scale is used for the RMSEs (y-axis) for demonstration purposes in (c).

When the influence of slopes was discussed, the aspect distribution of the 200 chosen GPS measurements should be as uniform as possible, and vice versa. Finally, the SRTM DEM was corrected based on these chosen in situ measurements using the proposed method.

Figures 7(b) and 7(c) show the RMSEs of the corrected SRTM DEM using in situ GPS measurements with different slope and aspect distributions. As shown in Figure 7(b), the RMSE is approximately 198.2 m when in situ measurements with a slope threshold smaller than 5° (nearly flat) were used. When the slope threshold increased to 35° , the RMSE exponentially decreased to approximately 9.4 m. Then, the RMSE slightly decreased until it remained stable at approximately 8.1 m. In addition, Figure 7(c) shows that the RMSE was approximately 5031.3 m when the aspect threshold was designated as 60° . Such a large RMSE indicates that the SRTM DEM correction failed in this case. In fact, this result is expected because the in situ measurements with aspects smaller than 60° have difficulty constraining the highly nonlinear errors with respect to the aspects (four orders in this study, see Figure 3(b)), resulting in significant errors in model parameter estimates relating to the aspects. Due to the aspect-related high-order nature in the constructed model (see Equation (7)), the error in the model parameter estimates would be dramatically magnified and forward propagated to the corrected SRTM DEM (causing an incorrect result). However, if the aspect threshold was set to 360° (i.e., covering all aspect ranges), the RMSE dramatically decreased to approximately 8.1 m. This result suggests that it is important to select uniformly distributed in situ measurements along the slope and aspect ranges of the ROI, especially for those areas with high-order errors relating to aspects and/or slopes.

V. CONCLUSIONS

This paper presents an adaptive method for simultaneously correcting the global error trends and the local linear/nonlinear terrain-related errors of the SRTM DEM. The test over the Zhangjiajie area of China shows that the RMSE of the corrected SRTM DEM is approximately 8.1 m, indicating an improvement of approximately 20% with respect to the original result. In addition, we compared the corrected results with two common methods, namely, the SHM and MLE methods, that separately correct the global error trends and local linear terrain-related errors of the SRTM DEM. The results show average improvements of approximately 18.2% and 16.5%. In regard to mountainous areas with slopes larger than 20° , the accuracy improvements reach approximately 29% and 27.9%. This finding suggests that the proposed method is feasible and exhibits better accuracy performance compared with the previous SHM and MLE methods. Finally, we analysed the influence of gross errors, the number, and spatial distribution of in situ measurements. The results suggest that, owing to the utilization of robust estimation, the gross errors can be effectively mitigated if the percent ratio of gross errors ranges from 0% to 6%. Furthermore, a large number of in situ measurements with uniform slope

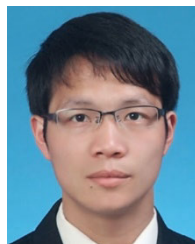
and aspect distributions is beneficial to improve the accuracy of the corrected SRTM DEM. Consequently, more possible measurements should be collected when the proposed method is used for SRTM DEM correction in practice.

However, we should stress that only the SRTM DEM in a small area (about 1200 km²) was selected to test the proposed method. Therefore, testing the proposed method in a large area (e.g., regional or even continental scale) will be our future topics. In addition, we will focus on the capability and performance analysis of the proposed method for SRTM DEM error correction under different land uses and terrain characteristics, in order to better guide the practical application scopes.

REFERENCES

- [1] T. Tadono, J. Takaku, K. Tsutsui, F. Oda, and H. Nagai, "Status of 'ALOS World 3D (AW3D)' global DSM generation," in *Proc. IEEE Int. Geosci. Remote Sens. Symp. (IGARSS)*, Jul. 2015, pp. 3822–3825.
- [2] T. Tachikawa, M. Hato, M. Kaku, and A. Iwasaki, "Characteristics of ASTER GDEM version 2," in *Proc. IEEE Int. Geosci. Remote Sens. Symp.*, Jul. 2011, pp. 3657–3660.
- [3] T. G. Farr, P. A. Rosen, E. Caro, R. Crippen, R. Duren, S. Hensley, M. Kobrick, M. Paller, E. Rodriguez, L. Roth, and D. Seal, "The shuttle radar topography mission," *Rev. Geophys.*, vol. 45, p. 2, Jun. 2007.
- [4] M. Zink, M. Bachmann, B. Brautigam, T. Fritz, I. Hajnsek, A. Moreira, B. Wessel, and G. Krieger, "TanDEM-X: The new global DEM takes shape," *IEEE Geosci. Remote Sens. Mag.*, vol. 2, no. 2, pp. 8–23, Jun. 2014.
- [5] Y. Yang, S. Jeong, L. Hu, H. Wu, S. W. Lee, and Y. Cui, "Transparent lithium-ion batteries," *Proc. Nat. Acad. Sci. USA*, vol. 108, no. 32, pp. 13013–13018, 2011.
- [6] Y. Zhou, Z. Li, J. Li, R. Zhao, and X. Ding, "Geodetic glacier mass balance (1975–1999) in the central Pamir using the SRTM DEM and KH-9 imagery," *J. Glaciol.*, vol. 65, no. 250, pp. 309–320, Apr. 2019.
- [7] K. Roback, M. K. Clark, A. J. West, D. Zekkos, G. Li, S. F. Gallen, D. Chamlagain, and J. W. Godt, "The size, distribution, and mobility of landslides caused by the 2015 Mw7.8 gorkha earthquake, nepal," *Geomorphology*, vol. 301, pp. 121–138, Jan. 2018.
- [8] V. Vanthof and R. Kelly, "Water storage estimation in ungauged small reservoirs with the TanDEM-X DEM and multi-source satellite observations," *Remote Sens. Environ.*, vol. 235, Dec. 2019, Art. no. 111437.
- [9] C. P. Sarma, A. Dey, and A. M. Krishna, "Influence of digital elevation models on the simulation of rainfall-induced landslides in the hillslopes of guwahati, india," *Eng. Geol.*, vol. 268, Apr. 2020, Art. no. 105523.
- [10] L. Ke, C. Song, B. Yong, Y. Lei, and X. Ding, "Which heterogeneous glacier melting patterns can be robustly observed from space? A multi-scale assessment in southeastern tibetan plateau," *Remote Sens. Environ.*, vol. 242, Jun. 2020, Art. no. 111777.
- [11] Q. Wu, C. Song, K. Liu, and L. Ke, "Integration of TanDEM-X and SRTM DEMs and spectral imagery to improve the large-scale detection of opencast mining areas," *Remote Sens.*, vol. 12, no. 9, p. 1451, May 2020.
- [12] E. Rodríguez, C. S. Morris, and J. E. Belz, "A global assessment of the SRTM performance," *Photogrammetric Eng. Remote Sens.*, vol. 72, no. 3, pp. 249–260, Mar. 2006.
- [13] S. Mukherjee, P. K. Joshi, S. Mukherjee, A. Ghosh, R. D. Garg, and A. Mukhopadhyay, "Evaluation of vertical accuracy of open source digital elevation model (DEM)," *Int. J. Appl. Earth Observ. Geoinf.*, vol. 21, pp. 205–217, Apr. 2013.
- [14] Y. Gorokhovich and A. Voustianiouk, "Accuracy assessment of the processed SRTM-based elevation data by CGIAR using field data from USA and thailand and its relation to the terrain characteristics," *Remote Sens. Environ.*, vol. 104, no. 4, pp. 409–415, Oct. 2006.
- [15] E. Berthier, Y. Arnaud, C. Vincent, and F. Rémy, "Biases of SRTM in high-mountain areas: Implications for the monitoring of glacier volume changes," *Geophys. Res. Lett.*, vol. 33, no. 8, 2006, Art. no. L08502.
- [16] D. J. Weydahl, J. Sagstuen, Ø. B. Dick, and H. Rønning, "SRTM DEM accuracy assessment over vegetated areas in norway," *Int. J. Remote Sens.*, vol. 28, no. 16, pp. 3513–3527, Aug. 2007.

- [17] Y. Su and Q. Guo, "A practical method for SRTM DEM correction over vegetated mountain areas," *ISPRS J. Photogramm. Remote Sens.*, vol. 87, pp. 216–228, Jan. 2014.
- [18] A. Wendleder, A. Felbier, B. Wessel, M. Huber, and A. Roth, "A method to estimate long-wave height errors of SRTM C-Band DEM," *IEEE Geosci. Remote Sens. Lett.*, vol. 13, no. 5, pp. 696–700, May 2016.
- [19] A. Kääh, "Combination of SRTM3 and repeat ASTER data for deriving alpine glacier flow velocities in the bhutan himalaya," *Remote Sens. Environ.*, vol. 94, no. 4, pp. 463–474, Feb. 2005.
- [20] F. E. O'Loughlin, R. C. D. Paiva, M. Durand, D. E. Alsdorf, and P. D. Bates, "A multi-sensor approach towards a global vegetation corrected SRTM DEM product," *Remote Sens. Environ.*, vol. 182, pp. 49–59, Sep. 2016.
- [21] Y. Su, Q. Guo, Q. Ma, and W. Li, "SRTM DEM correction in vegetated mountain areas through the integration of spaceborne LiDAR, airborne LiDAR, and optical imagery," *Remote Sens.*, vol. 7, no. 9, pp. 11202–11225, Sep. 2015.
- [22] A. Shortridge and J. Messina, "Spatial structure and landscape associations of SRTM error," *Remote Sens. Environ.*, vol. 115, no. 6, pp. 1576–1587, Jun. 2011.
- [23] L. Yue, H. Shen, L. Zhang, X. Zheng, F. Zhang, and Q. Yuan, "High-quality seamless DEM generation blending SRTM-1, ASTER GDEM v2 and ICESat/GLAS observations," *ISPRS J. Photogramm. Remote Sens.*, vol. 123, pp. 20–34, Jan. 2017.
- [24] L. Yue, H. Shen, L. Liu, Q. Yuan, and L. Zhang, "A global seamless DEM based on multi-source data fusion (GSDEM-30): Product generation and evaluation," 2019, Art. no. 2019060036, doi: [10.20944/preprints201906.0036.v1](https://doi.org/10.20944/preprints201906.0036.v1).
- [25] F. R. Hampel, "The influence curve and its role in robust estimation," *J. Amer. Stat. Assoc.*, vol. 69, no. 346, pp. 383–393, Jun. 1974.
- [26] P. J. Huber, "Robust estimation of a location parameter," *Ann. Math. Statist.*, vol. 35, no. 1, pp. 73–101, Mar. 1964.
- [27] J. W. Zhou, "Classical theory of errors and robust estimation," *ACTA Geodetica Cartogr. Sin.*, vol. 18, no. 2, pp. 115–120, May 1989.
- [28] D. Yamazaki, D. Ikeshima, R. Tawatari, T. Yamaguchi, F. O'Loughlin, J. C. Neal, C. C. Sampson, S. Kanae, and P. D. Bates, "A high-accuracy map of global terrain elevations," *Geophys. Res. Lett.*, vol. 44, no. 11, pp. 5844–5853, Jun. 2017.
- [29] X. Zhao, Y. Su, T. Hu, L. Chen, S. Gao, R. Wang, S. Jin, and Q. Guo, "A global corrected SRTM DEM product for vegetated areas," *Remote Sens. Lett.*, vol. 9, no. 4, pp. 393–402, Apr. 2018.



ZEFA YANG (Member, IEEE) received the bachelor's and Ph.D. degrees in surveying engineering from the China University of Mining and Technology, Xuzhou, and Central South University, Changsha, China, in 2011 and 2018, respectively.

From October 2015 to 2017, he was an exchanging Ph.D. candidate in geodesy and survey engineering with RWTH Aachen University, Aachen, Germany. He is currently a Full Professor with the Department of Surveying and Remote Sensing, School of Geosciences and Info-Physics, Central South University. His research interests include interferometric synthetic aperture radar (InSAR) and its applications for monitoring and modeling ground surface deformation associated with underground extraction. He has published more than 20 articles in international peer-reviewed journals.



MINSI AO received the B.S. and M.S. degrees in communication engineering and the Ph.D. degree in geographic information engineering from the China University of Geosciences, Wuhan, China, in 2007, 2009, and 2012, respectively. From 2012 to 2014, he has finished the postdoctoral research with Central South University, Changsha, China. He is currently a Senior Engineer and the Deputy of the Hunan Continuously Operating Stations Data Center, Hunan Institute of Geomatics Science and Technology. He is also the M.S. Instructor of the School of Geosciences and Info-physics, Central South University. His research interests include the global navigation satellite system technology and its application, and geodetic datum and its maintenance.

Dr. Ao received the First Prize of Hunan provincial scientific and technology progress in geomatics, from 2015 to 2018 (Hunan Society of Geomatics Science and Technology) and the second level of national scientific and technological progress in surveying and mapping, in 2018 (Chinese Society for Geodesy, Photogrammetry and Cartography).



CUI ZHOU was born in Shaoyang, Hunan, China, in 1982. She received the B.Eng. degree in computer and the M.Agr. degree in information engineering from the Central South University of Forestry and Technology, China, in 2005 and 2010, respectively, and the Ph.D. degree in surveying science and technology from Central South University, China, in 2015.

Since 2005, she has been with the Central South University of Forestry and Technology, where she is currently a Professor in geography. Her current research and interest areas include surveying adjustment, image registration, and super-resolution image reconstruction.

Dr. Zhou awards and honors include outstanding talent in Hunan Province, China, and ents scholars in the Central South University of Forestry and Technology.



GUI ZHANG was born in Yiyang, Hunan, China, in 1964. He received the B.S. degree in mathematics from Hunan Normal University, China, in 1986, and the M.Agr. and Ph.D. degrees in forestry information engineering from the Central South University of Forestry and Technology, China, in 1994 and 2004, respectively.

Since 1985, he has been with the Central South University of Forestry and Technology, where he is currently a Professor in forest management. His current research and interest areas include forestry information engineering, forest fire ecology, and satellite applications in disaster prevention and reduction.

Dr. Zhang awards and honors include outstanding Hunan new century 121 talents project talents and Hunan Province public emergency management experts.



ZHIWEI LIU received the B.S. degree in surveying and mapping engineering from the Changchun Institute of Technology, Jilin, China, in 2015, and the M.S. degree in geodesy and surveying engineering from Central South University, Changsha, China, in 2019, where he is currently pursuing the Ph.D. degree with the School of Geosciences and Info-physics. His current research mainly focuses on the interferometric synthetic aperture radar on DEM generation.



JIANJUN ZHU received the M.Eng. degree in engineering surveying and the Ph.D. degree in geodesy and surveying engineering from the Central South University of Technology (currently Central South University), Changsha, China, in 1985 and 1998, respectively. In 1998 and 1999, he was a Research Assistant with the Department of Land Surveying and Geo-informatics, The Hong Kong Polytechnic University, Hong Kong. From 2000 to 2001, he was a Postdoctoral Fellow

with the Center for Research on Geomatics, Laval University, Quebec City, QC, Canada. He is currently a Full Professor with the School of Geosciences and Info-Physics, Central South University. His research interests include the theory of errors and surveying adjustment and its applications on InSAR and GPS.

...